INSTITUT DE FRANCE
Académie des sciences

Comptes Rendus
Chimie

Emna Rahali, Leila El-Bassi, Latifa Bousselmi, Marta M. Alves, Maria de Fátima Montemor and Hanene Akrout

Influence of sulfate-reducing bacteria on the biocorrosion of mild steel coated with hybrid polyetherimide-ZnO or CuO bilayer composites

Published online: 11 April 2023

https://doi.org/10.5802/crchim.227

Part of Special Issue: Materials and Clean Processes for Sustainable Energy and Environmental Applications

Guest editors: Mejdi Jeguirim (Université de Haute-Alsace, Institut de Sciences des Matériaux de Mulhouse, France) and Patrick Dutournié (Université de Haute-Alsace, Institut de Sciences des Matériaux de Mulhouse, France)

Les Comptes Rendus. Chimie *sont membres du*
Centre Mersenne pour l'édition scientifique ouverte
www.centre-mersenne.org
e-ISSN : 1878-1543

Comptes Rendus
Chimie
Published online: 11 April 2023
https://doi.org/10.5802/crchim.227

Materials and Clean Processes for Sustainable Energy and Environmental Applications /
Matériaux et procédés propres pour des applications énergétiques et environnementales

Influence of sulfate-reducing bacteria on the biocorrosion of mild steel coated with hybrid polyetherimide-ZnO or CuO bilayer composites

Influence des bactéries sulfato-réductrices sur la biocorrosion de l'acier doux revêtu de composites bicouches hybrides polyétherimide-ZnO ou CuO

Emna Rahali[a, b], Leila El-Bassi[*, a], Latifa Bousselmi[a], Marta M. Alves[c], Maria de Fátima Montemor[c] and Hanene Akrout[a]

[a] Laboratory for Wastewater and Environment, Water Researches and Technologies Center (CERTE), Technopark of Borj Cedria, PB 273, Soliman 8020, Tunisia

[b] National Institute of Applied Science and Technology (INSAT), Carthage University, Tunis, Tunisia

[c] Centro de Química Estrutural, Institute of Molecular Sciences, Departamento de Engenharia Química, Instituto Superior Técnico, Universidade de Lisboa, Av. Rovisco Pais 1049-001, Lisboa, Portugal

E-mails: rahali93@hotmail.com (E. Rahali), l.elbassi@gmail.com (L. El-Bassi), latifa.bousselmi.certe@gmail.com (L. Bousselmi), marta4alves@gmail.com (M. M. Alves), mfmontemor@tecnico.ulisboa.pt (M. F. Montemor), Hanene.akrout@yahoo.com (H. Akrout)

Abstract. Mild steel (MS) coated with protective bilayer hybrid coatings of polyetherimide, and ZnO/CuO was exposed to artificial treated wastewater (ATWW) inoculated with *Desulfovibrio* sp. (biotic system). Proteins from the extracellular polymeric substances (EPS) matrix of *Desulfovibrio* sp. responded to the coatings. PEI-CuO offered the highest performance against biocorrosion. The higher PEI-CuO resistivity value of 2.17×10^6 Ω·cm^2 contrasted with the decrease to 1.5×10^5 and 1.6×10^3 Ω·cm^2 for PEI-ZnO and PEI coatings, respectively. The one order of magnitude increased resistance of the biotic system, compared to sterilized ATWW (abiotic system), resulted from the protective nature of the bacterial biofilm.

* Corresponding author.

Résumé. L'acier doux (MS) recouvert de revêtements hybrides bicouches protecteurs de polyétherimide et de ZnO/CuO a été exposé à des eaux usées artificielles (ATWW) inoculées par *Desulfovibrio* sp. (système biotique). Les protéines de la matrice des substances polymères extracellulaires (EPS) de *Desulfovibrio* sp. ont réagi aux revêtements. Le PEI-CuO a offert les meilleures performances contre la biocorrosion. La valeur de résistivité plus élevée de PEI-CuO de $2{,}17 \times 10^6$ $\Omega{\cdot}cm^2$ contraste avec la diminution à respectivement $1{,}5 \times 10^5$ et $1{,}6 \times 10^3$ $\Omega{\cdot}cm^2$ pour les revêtements PEI-ZnO et PEI. La résistance accrue d'un ordre de grandeur du système biotique, par rapport à l'ATWW stérilisé (système abiotique), résulte de la nature protectrice du biofilm bactérien.

Keywords. Biocorrosion, *Desulfovibrio* sp, Oxide, EPS, Inhibition.

Mots-clés. Biocorrosion, *Desulfovibrio* sp, Oxyde, EPS, Inhibition.

Published online: 11 April 2023

1. Introduction

Due to its composition, wastewater is the most complex matrix that favors microbial growth on several metal surfaces under short periods, particularly on steel commonly used in industrial equipments [1]. It comprises two fractions, an organic and an inorganic one. The former is mainly composed of carbohydrates, proteins, lipids and industrial residues, where as phosphorus, chlorides, nitrogen, and limited amounts of heavy metals comprise the latter fraction [2]. In fact, microorganisms adhere to the steel surface where they colonize, reproduce and finally form a biofilm, affecting the kinetics of the cathodic and anodic corrosion processes [3–5]. This phenomenon is called biocorrosion or microbiologically influenced corrosion (MIC) [6].

Well-known microorganisms in steel biocorrosion are the sulfate-reducing bacteria (SRB) [7–9]. SRB can aerobically produce sulfide from sulfate and thiosulfate reduction [10], which is considered as the highest risk factor in biocorrosion processes [7–11]. Besides, SRB can use O_2 and Fe^{3+} and oxidize hydrogen; they can also utilize aliphatic and aromatic hydrocarbons, and link sulfate reduction to intracellular magnetite production [10]. Furthermore, bacterial sessile cells within the SRB biofilm have the ability to harvest energy from SO_4^{2-} reduction for metabolic activities. Therefore, SRB can reduce SO_4^{2-} to HS^- and the Fe^{2+} generated by the anodic process then reacts with HS^- to form sulfide precipitates (FeS) in the biofilm. FeS is the typical corrosion product formed when mild steel (MS) is exposed to an environment containing SRB [12,13]. Chen *et al.* [14] proved that the presence of SRB in seawater could generate localized corrosion in carbon steel. The authors reported that the cathodic and anodic areas present different morphological features in the presence of SRB strain. In fact, the corrosion products formed in the cathodic area were more compact than those grown in the anodic areas. Likewise, Li *et al.* [15] studied bacterial distribution in SRB biofilms. They showed that SRB bacteria could generate both forms of corrosion: localized and uniform, and that bacterial distribution in biofilms varied, depending on the type of corrosion. In the presence of localized corrosion, bacterial cells were distributed at the bottom of the biofilm, whereas in generalized corrosion, cells gathered outside the SRB biofilm [15].

Apart from SO_4^{2-}, chlorides present in the wastewaters are critical for pitting formation [16]. El-Bassi *et al.* [16] investigated the effect of chloride in the biocorrosion of carbon steel immersed in wastewaters. They reported that pitting is one of the primary forms of corrosion caused by this anion [16]. Ferrous ions react with the chlorides to form $Fe(OH)_2$ and consequently release H^+ and Cl^-. The described cycle is repeated until the protective layer of Fe_2O_3 or Fe_3O_4 is entirely abolished. In the presence of biofilm, oxidizing iron reacts with Cl^-, as follows (Equations (1) and (2)):

$$Fe^{2+} + 2Cl^- \leftrightarrows FeCl_2 \quad (1)$$

$$FeCl_2 + 2H_2O \leftrightarrows Fe(OH)_2 + 2H^+ + 2Cl^- \quad (2)$$

In this context, Ziadi *et al.* [12] reported that SRB could induce pitting corrosion in the first stage of biocorrosion on stainless steel immersed in wastewater, which produced hydrogen sulfide (H_2S) or iron sulfide (FeS_2) by SO_4^{2-} reduction [12]. Rajala *et al.* [17] investigated carbon steel biocorrosion in anoxic groundwater containing SRB and methanogenic archaea (MA) [17]. They reported that the corrosion rate in abiotic system (1 μm/y) was the lowest among the studied systems; however, in biotic environments, the corrosion rates (between 5 μm/y and 10 μm/y) are higher in SRB-enriched environments and lower in SRB and MA environments [17].

Among the SRB group, several studies investigated the impact of *Desulfovibrio* sp. on steel in different environments [18,19]. Wikie *et al.* [20] evaluated the negative effect of *Desulfovibrio Alaskensis* sp. biofilms on the corrosion progress of carbon steel in marine environments. The biofilm that settled on the MS surface was a complex structure composed mainly of bacteria, metallic ions, extracellular polymeric substances (EPS), and biocorrosion products [21,22].

Polymeric coatings are relevant in preventing corrosion, particularly to overcome microbiologically influenced corrosion (MIC). This strategy is of primary relevance when the coatings are composed of non-toxic substances such as polyetherimide (PEI) [23]. Two essential factors should be considered when selecting additives for coatings' design, which are (i) high resistance to bacterial attack and (ii) absence of corrosion products formation as a result of the coating degradation [24]. To enhance the protectiveness of coatings in treated wastewaters, several metal oxides, like TiO_2, have been tested as microbial growth inhibitors as possible alternatives to traditional and toxic biocides [25]. Ziadi *et al.* [12] demonstrated that incorporating TiO_2 nanoparticles in a silane coating can mitigate biocorrosion of stainless steel in contact with treated urban wastewaters [12].

Zinc and copper oxides have shown antibacterial effectiveness in several applications [26,27]. Thus, metal oxide additives for antimicrobial polymers are considered safe solutions with high antibacterial efficiency, and improved polymer stability and maintenance of its functional properties [28].

Previously, Rahali *et al.* [29] studied the impact of hybrid coatings on the corrosion progress of MS in simplified abiotic environments (3.5 wt% NaCl) and reported that the corrosion resistance of MS was enhanced by ZnO and CuO, leading to a protective efficiency equal to 70% and 99%, respectively. This good efficiency is probably due to the higher coating thickness and smaller pores present in the outer layer [29]. The proven efficiency for MS corrosion protection in abiotic environments makes these coatings worthy of exploring in complex biotic environments.

Thus, the present work aims to understand the biocorrosion progression of MS coated with hybrid PEI composite bilayers in the presence of ZnO or CuO. To reach this objective, uncoated and coated MS samples were exposed to a biotic system simulated by ATWW inoculated with *Desulfovibrio* sp. The biofilm and the EPS layers were characterized, namely the polysaccharide, protein and lipid contents. The relationship between these layers' compositions and the coatings is discussed. The protectiveness of the coatings in the biotic system was compared with an abiotic system (sterilized artificial treated wastewater, SATWW). This protectiveness was assessed using electrochemical impedance spectroscopy (EIS) and through a deep physicochemical analysis of the corrosion layers formed on the bare and coated MSsurface.

2. Materials and methods

2.1. *Bacterial strain and cultivation conditions*

The strain *Desulfovibrio* sp. (MK782593), used as a model of SRB, was isolated from a previous study [30]. Briefly, for cultivation and isolation of *Desulfovibrio* sp., the biofilm formed on the surface of 304 L SS immersed in treated urban wastewater was collected after 3 days of immersion. The biofilm collected was cultivated in SRB selective medium (consisting of 0.5 g of K_2HPO_4, 1.0 g of NH_4Cl, 0.5 g of Na_2SO_4, 0.1 g of $CaCl_2$, 2.0 g of $MgSO_4$, 3.5 g of $C_3H_5NaO_3$ and 1.0 g of ascorbic acid in 1 L of distilled water at pH 7.20 ± 0.02).

The inoculated medium was incubated at 30 °C for 21 days when black deposits and hydrogen sulphide odour were detected. After this period, SRB suspensions were cultivated on Petri dishes in the presence of nutrient agar. Isolation consisted of three successive subcultures of each strain and then inoculation into liquid media. Before use, the strain *Desulfovibrio* sp. was re-cultivated in SRB selective medium. Bacterial inoculation was carried out using a cell suspension at the exponential growth phase [12].

2.2. *Preparation of mild steel (MS) coupons*

DC01 carbon steel (CS) with chemical composition (wt%): C < 0.12; Mn < 0.60; P < 0.045; S < 0.045. Steel coupons (2.5 cm × 2.5 cm) were abraded with silicon carbide (SiC) papers of 230, 320, 600, 1000, and 1200 grit and rinsed with distilled water. Finally, samples were degreased with ethanol in an ultrasounds bath and dried with an air stream.

2.3. *Synthesis of sol–gel coating*

As previously described, the hybrid coating was composed of two layers applied in separate steps [29]. Briefly, the first polymeric layer was synthesized by mixing PEI (Sigma-Aldrich) in 15% N,N-dimethylacetamide (DMAc, Fluka). The coating was applied by dip-coating, employing a dip coater RSC15 (Bungard Elektronik) controlled by a SIEMENS SPS unit. The coated samples were cured in an oven for 4 h at 160 °C. The second layer was synthesized precisely as the previous one, where CuO or ZnO particles (0.123 g/L) were added to the polymeric solution.

2.4. *Coupons incubations with Desulfovibrio sp. strain*

Anaerobic vials (250 mL) were filled with 100 mL ATWW (Table S1). Bare and coated steel coupons were added to each vial before inoculation. Then, each vial was inoculated with 100 µL of overnight cultivation of SRB suspension ($O.D._{660\ nm} \sim 1$). The coupons were sampled after 7 days of immersion, gently washed, and used for microbiological characterization.

2.4.1. *Extracellular polymeric substances (EPS) extraction and characterization*

Bacterial biofilms from the SRB strain were recovered from the MS surface immersed in artificial urban wastewaters. The recovered biofilm was washed with 0.9 wt% NaCl, and suspended in a 5 mL saline solution (0.9 wt% NaCl). Biofilm suspensions were then centrifuged at 12,000 rpm for 20 min at 4 °C to obtain the EPS supernatant. EPS extraction was performed according to the method previously described by Liu *et al.* [31], using EDTA (2%) as an extractant. Briefly, 1 mL of EDTA was added to each test tube with biofilm suspension and rested for 3 h at 4 °C. The resulting suspension was filtered through a 0.2 µm membrane, followed by a dialysis membrane filtration (3500 Da). The obtained filtrates were lyophilized for 48 h at −50 °C, and the recovered EPS was quantified using an electronic balance [31].

The polysaccharide content of EPS was determined using the phenol-sulfuric acid assay with glucose as standard [32]. The protein content of EPS was measured by the Bradford assay using casein as the standard [33]. The sulfo-phospho-vanillin method was used to determine the lipid content [34]. All EPS analysis was performed in duplicate.

2.4.2. *Surface characterization*

The morphological observation of the bare and coated samples before and after immersion in ATWW, with or without bacteria, was characterized using scanning electron microscopy (SEM) (PhenomProX G6, JEOL-JSM7001F). The X-ray energy dispersive spectrometer (EDS) was used to assess the elemental chemical composition. The conductivity of the samples was improved with a thin coating of conductive gold/palladium (Polaron E-5100).

An optical camera assessed the water contact angle on the immersed coated surfaces. In brief, a droplet of water of ~5 µL was placed on the coating surface using a tension meter (AttentionTheta T200).

2.4.3. *Electrochemical measurements*

The electrochemical impedance spectroscopy (EIS) technique was used to investigate the interface behaviors of the bare and coated MS in both biotic and abiotic systems using an experimental setup with a three electrodes conventional cell. A potentiostat Voltalab PGZ301 was used. EIS measurements were undertaken at open circuit potential (E_{oc}), under a sinusoidal perturbation of ±10 mV for frequencies ranging from 65 kHz to 10 mHz, with an acquisition frequency of 10 points per decade. The EIS measurements were performed after 7 days. Each experiment was conducted in duplicate. The experimental impedance spectra were analyzed and fitted using the Zsimpwin version 3.30d (EChemSoftware, Ann Arbor, MI, USA) with suitable equivalent circuit models; to ensure the fitting reliability, only regressions with a chi-square of $\leq 10^{-3}$ were accepted.

2.4.4. *Statistical analyses*

Both the values of the amount and relative composition of the EPS content are averaged values of at least three measurements, and the error bars represent their standard deviations.

3. Results and discussions

3.1. *Desulfovibrio sp. biofilms formed on bare and coated MS immersed in artificial treated wastewater*

Following the efficacy of PEI-ZnO and PEI-CuO to protect MS under simplified biotic conditions

(3.5 wt% NaCl) [29], the coatings were tested in quasi-real conditions. Artificial treated wastewater (ATWW) with bacteria was selected as a biotic system model in this studyand was compared with an abiotic system of sterilized ATWW (SATWW).

SEM observations were used to characterize the surface of MS, PEI, PEI-ZnO, and PEI-CuO before and after immersion in ATWW with or without *Desulfovibrio* sp. (Figure S1, Figure 1).

Figure 1a–d shows the morphological features of the biofilm formed on bare and coated MS in *Desulfovibrio* sp. inoculated media. An abiotic assay was performed using the above-indicated coating but without SRB strain inoculation (Figure 1e–h). In this medium, only corrosion products are noticed on the steel surface (Figure 1e–h), contrasting with the biotic medium where corrosion products and individualized SRB cells can be clearly detected (Figure 1a–d). Similar results were attained by Rasool *et al.* [35]. In particular, the observation of the bare MS surface 7 days after immersion (Figure 1a) shows an adherent homogeneous biofilm, confirming the easiness of SRB to establish and progress to a biofilm. In PEI-coated MS (Figure 1b–d), the SEM observation shows fewer bacterial colonies scattered on the surface. Changes in bacterial colonization could be related to differences between MS and MS/PEI surfaces in terms of structure and/or physicochemical properties of PEI.

The roughness in the PEI coating can influence the dynamic of biofilm development and other microbial interactions. Aguirre *et al.* [36] reported that electrostatic adherence between coatings and microorganisms could lead to leakage of microbial contents and disruption of the cell wall.

A more heterogeneous structure for the biofilm (Figure 1c) was observed on the coated MS after immersion for the PEI-ZnO coating. An obvious deformation on the bacterial biofilm surface occurred compared to the non-coated steel (Figure 1a). This damage could be attributed to the bactericide effect of PEI-ZnO, which altered the homogeneity of the deposited bacterial biofilm. Rasheed *et al.* [37] demonstrated that chitosan-ZnO_{NPs} (CZNC-10) coatings on carbon steel had an inhibitory effect on SRB biofilm establishment after 7 days of incubation, with a significant biofilm deformation. This deformation may be due to the inhibition efficiency of chitosan-ZnO_{NPs}, which makes the SRB more susceptible to damage [37]. The antibacterial activity of ZnO has been proven by several studies [38]. Malini *et al.* [39] revealed that the presence of ZnO in membranes blocked biofilm formation and demonstrated antifouling activity on wastewater filtration membranes. In addition, Dhillon *et al.* [40] noted strong anti-biofilm activity of chitosan-ZnO_{NPs} against *Staphylococcus aureus* and *Micrococcus luteus even* when small concentrations of ZnO nanoparticles were added. The antibacterial activity of ZnO is based on the interaction of the particles with bacteria.This interaction leads to the release of Zn^{2+} and causing to the deterioration of bacterial cell walls, lipids, proteins and DNA [41].

A pronounced bactericide effect was observed with the PEI-CuO coating (Figure 1d), in which the number of SRB individual colonies was significantly decreased with a notable complicated and porous structure. The literature demonstrates that CuO had a bactericide effect on *Desulfovibrio marinisediminis* GSR3 strain and on *Pseudomonas aureus* by inactivating the catabolic metabolism and biosynthesis mechanismson the latest [42–44].

Fathy *et al.* [45] investigated styrene N-vinylpyrrolidone nanocomposites' efficiency when combined with a metal oxide (CuO or ZnO) against SRB-induced biocorrosion. Authors demonstrate that the SRB biocidal activity on coated MS was higher for the copolymer/ZnO (3%) and CuO (0.3%) coatings [45]. According to the literature [29–46], the abrasive surface shape of ZnO and CuO particles can destroy bacterial membranes. Also, the presence of Zn^{2+} and Cu^{2+} from particles can be a possible variant of antibacterial activity, as these cations can disrupt amino acid metabolisms, enzyme systems and transport of substances into cells, subsequently inhibiting bacterial cell growth [47].

The altered biofilm structure and corrosion products layer (biolayer), influenced by the metal oxides in the coatings, affects the surface properties of both bare and coated metal. If, on the one hand, it is possible to predict bacterial adhesion by the water contact angle (WCA) analysis of the coatings, on the another hand, it is possible to assess the biocorrosion progression by analysing the WCA of the biolayers formed over these coatings. WCA measurements were used to assess such alterations, as presented in (Figure 2).

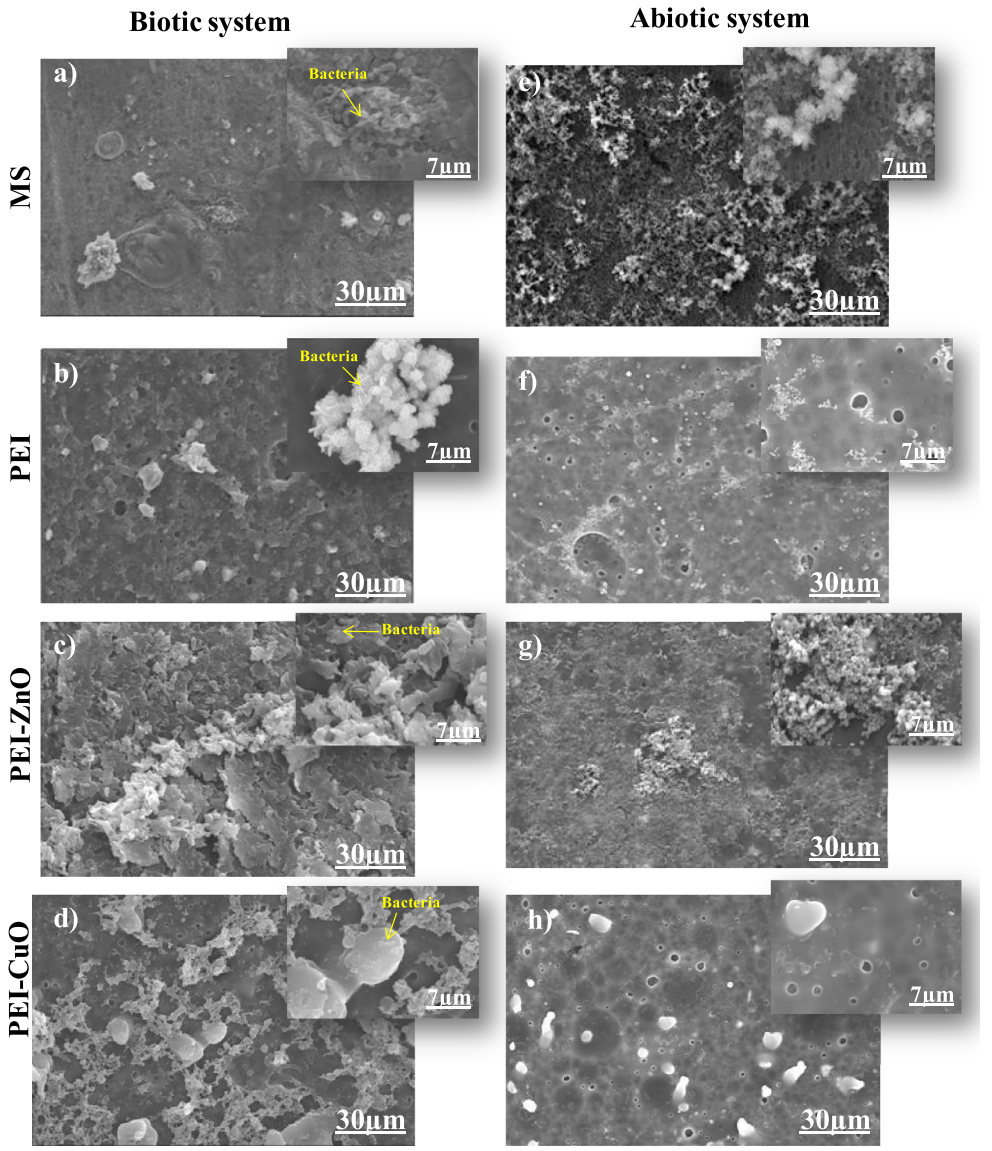

Figure 1. Top view SEM images of (a) MS, (b) PEI, (c) PEI-ZnO and (d) PEI-CuO immersed in biotic system, (e) MS, (f) PEI, (g) PEI-ZnO and (h) PEI-CuO immersed in abiotic system; insets are magnified SEM images.

Based on previous work [29], WCA values for PEI and PEI-coatings are recorded at 84° and increased to 92° in the presence of CuO [29]. According to the literature, the hydrophobicity of a surface is a major factor governing bacterial adhesion [48]. However, the importance of this parameter is related to the type of bacteria [49]. In fact, hydrophilic bacteria like *Desulfovibrio desulfuricans* prefer to adhere to hydrophilic surfaces [50]. Chen *et al.* [50] reported that an increase in the hydrophobicity of the CS surface resulted in a remarkable reduction of SRB adhesion. This trend was not verified as bare MS, with the highest WCA, was the surface with more bacteria. In contrast, the PEI-CuO coating, with the highest WCA amongst the coatings, had few bacterial adhesions (Figure 2). This was further proved by the hydrophilicity of the layers formed on bare and coated MS when immersion in the biotic system.

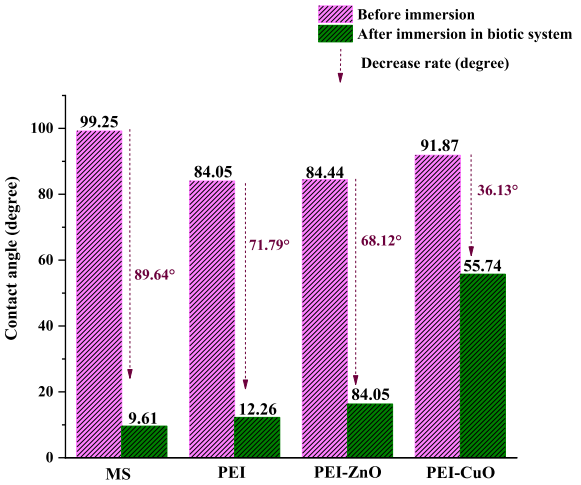

Figure 2. Water contact angles of bare and coated steel before and after immersion in biotic system; the contact angle of samples before immersion are taken from the authors' previous work [29].

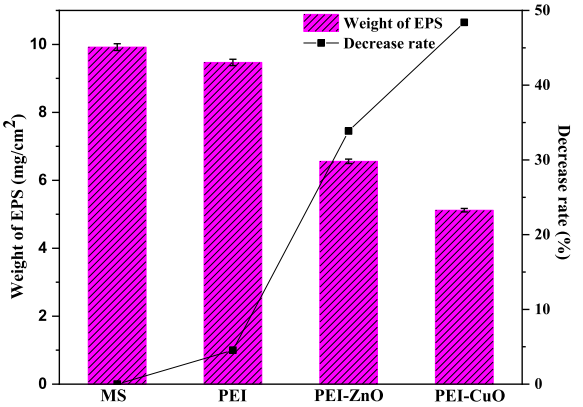

Figure 3. EPS weights (mg) obtained of the biofilm grown on bare and coated mild steel after 7 days of immersion in the biotic system.

Upon immersion in ATWW with *D. desulfuricans*, it was noticed that WCA were dramatically decreased (Figure 2). This decrease can be due to the type of biolayer form on MS in this medium [51]. These biolayers caused a decrease in the WCA of approximately 90° for the bare MS, 72° for PEI, 68° for PEI-ZnO and 36° for the PEI-CuO coatings (Figure 2). These findings are in line with the decreased biofilm and corrosion products formation on bare MS > PEI > PEI-ZnO > PEI-CuO (Figures 1 and 2).

3.2. *Impact of Desulfovibrio sp. on EPS production and characterization*

To further explore SRB settling, the production of EPS, a key component in evaluating microbial growth and bacterial biofilm establishment on surfaces, was studied [30]. Thus, further EPS-produced biofilm characterization was made to assess the coating effect on the bacterial biofilm. It is worth mentioning that the presence of SRB strain is well recognized to enhance EPS production, which facilitates biofilm adhesion and shows its ability to produce EPS, even under small biomass concentrations [37–52].

Figure 3 reports the EPS yields extracted from biofilms grown on the different coated and bare MS surfaces after 7 days of immersion in ATWW with *Desulfovibrio* sp. The produced EPS mass was more relevant in the case of the uncoated MS (Figure 3). In the case of the PEI coating, a decrease in EPS mass of about 4% was observed compared to the non-coated MS (Figure 3), indicating that the PEI coating was not primarily affecting EPS production by *Desulfovibrio* sp. Previous studies demonstrated that PEI does not exhibit bactericide activity [11,53] and suggest that the decrease in biofilm production in the presence of PEI maybe somehow related to anti-adherence mechanisms rather than direct biocidal effects [11].

In the case of PEI-ZnO and PEI-CuO coatings, EPS production decreased compared to the bare MS, about 34% and 48%, respectively (Figure 3). When added to PEI, Zn or Cu oxides had a notable decrease rate on the EPS weight (Figure 3), but it was not completely inhibited. In fact, the ZnO-PEI composite exhibits high inhibition rates against *S. aureus* and *E. coli* even after being subjected to harsh simulated conditions [53].

Hewayde *et al.* [54] investigated the toxicity of CuO to SRB. The concrete sewer pipes coated with CuO exhibited antimicrobial characteristics against *Desulfovibrio desulfricans* isolated from a lab-scale anaerobic digester and showed 99% inhibition against bacteria as well as in their EPS production. While the EPS production observed in our work aligns with Hewayde's *et al.* [54] report, other points in the opposite direction of EPS enhanced production to preserve the inner microorganisms from harsh external environmental conditions [19,20]. Fang *et al.* [55]

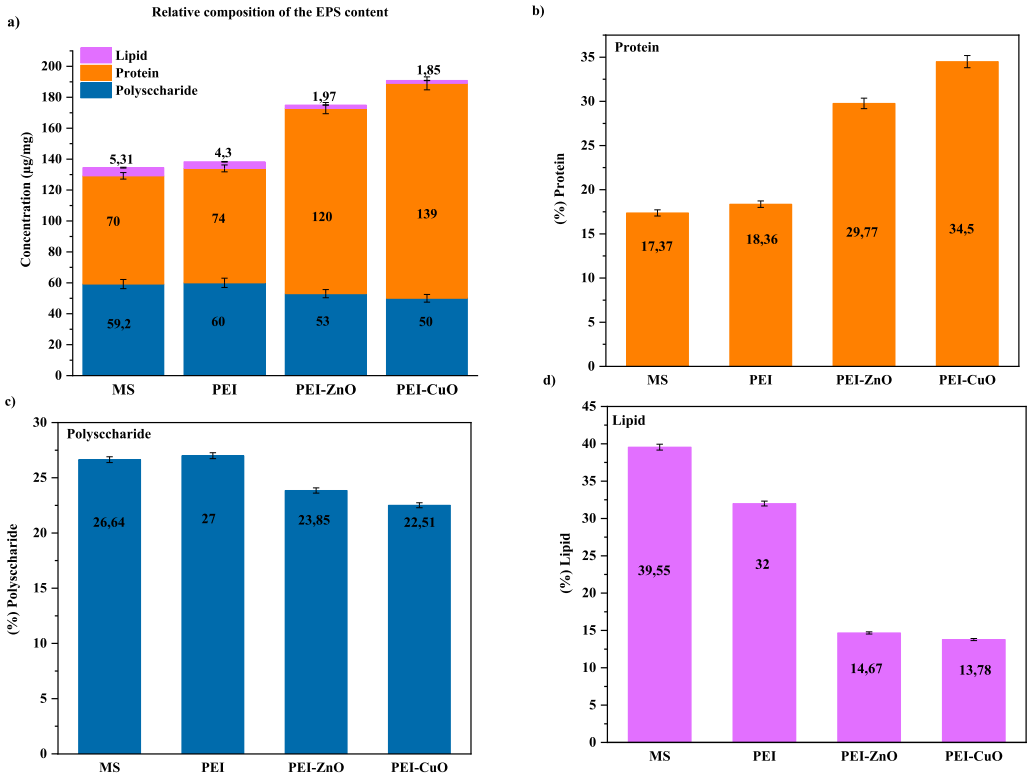

Figure 4. (a) Relative composition of the EPS content and evolution of the EPS, (b) protein content, (c) polysaccharide and (d) lipid of the extracted EPS from the biofilm grown on bare and coated MS immersed in ATWW.

demonstrated Cu^{2+} as being the most toxic element to SRB among all tested metals and chemicals. In fact, exposure of SRB to Cu^{2+} slightly stimulated the production of EPS. Likewise, Miao *et al.* [56] demonstrated that the EPS content was considerably increased in response to CuO-nanoparticles exposure in wastewaters. Zn^{2+} proved less inhibitory to SRB activity, yet it greatly stimulated EPS production [55]. Yue *et al.* [57] investigated EPS production by *Desulfovibrio desulfuricans* strain when Cu^{2+} and Zn^{2+} were added to the culture medium. Authors demonstrated that the EPS extracted from bacteria exposed to Zn^{2+} increased the binding affinity for all heavy metals, therefore reducing the inhibitory impact of Cu^{2+} on the SRB [57]. A similar result was proved by Zhao *et al.* [58], where nano-ZnO's presence accelerated the EPS production from *Chlorella vulgaris*.

These contradictory data prompt us to investigate further the effect each coating caused on the EPS content (Figure 4). The content distribution of the EPS extracted from the *Desulfovibrio* sp. biofilm established on the coated MS is reported in Figure 4. Protein content represented the highest component among EPS contents (Figure 4a). The protein content was about 70 and 74 µg/mg for bare MS, and PEI-coated steel, respectively (Figure 4a), which underlined that the PEI coating did not impact protein production. The protein content increased to 120 and 139 µg/mg in the presence of PEI-ZnO and PEI-CuO coated MS (Figure 4a). The protein content increased in the presence of the different coatings to a maximum value of 34.5% for PEI-CuO coated steel. According to Figure 4c, the polysaccharide content is between 22% of the EPS content for PEI-CuO as a minimum value, and 27% for MS as the maximum value. So the addition of metal oxides to the coatings significantly increased protein content but caused a low variation in the polysaccharide content.

These results agree with Pérez *et al.* [59] that *Desulfovibrio* sp. proteins are the main constituents

of biofilms formed on CS when immersed in synthetic seawater. Also, Chen *et al.* [60] demonstrated that *Desulfovibrio vulgaris* counteracted CuO nanoparticles stress by increasing the protein content of EPS to protect bacterial biofilm from toxic elements [56,57]. Miao *et al.* [56] found a dominance of protein contents, compared to polysaccharides, in response to CuO nanoparticles. Likewise, EPS containing a higher amount of protein was reported in the presence of zinc oxide [58]. On the contrary, Yue *et al.* [57] demonstrated that Cu^{2+} and Zn^{2+} added to the culture medium of *Desulfovibrio desulfuricans* increased polysaccharides and reduced protein contents. This was explained by a modification in the carboxyl group of proteins and in the C–O–C group of polysaccharides contained in the EPS that caused an improved binding capacity of the metals [60].

In our specific case, the particles embedded within the coatings modified EPS production in such a way that protein production was favored over polysaccharide production, most probably due to the combination of PEI with Cu or Zn ions release.

The lipid content in the extracted EPS (Figure 4a) did not exceed 6 μg/mg for bare and coated steel. Bare MS has the highest lipid content, with a percentage of 39.5% (Figure 4c), while the lowest was detected for PEI-CuO (1.85 μg/mg). Conrad *et al.* [61] indicated that the lipid fraction impacts biofilm adhesion to the substrate and influences the hydrophobic properties of EPS. Thus, lipid fractions lead to the maintenance and establishment of biofilm structures [62]. Also, lipids may participate membranes and micelles formation, leading to Van Der Waals interactions in the biofilm [63]. The decreased lipid content on PEI-CuO might explain the damaged structure of biofilm observed by SEM imaging (Figure 1).

Liu and Fang [63] demonstrated that the hydrophilicity/hydrophobicity of EPS highly influences the hydrophobicity of the bacterial biofilm. The extracted EPS from PEI-CuO coating, in which the protein represents the main component of the total EPS (Figure 4), aligns with the high hydrophobicity observed over the formed biofilm (Figure 4).

3.3. *Impact of Desulfovibrio sp. biofilms on the corrosion behavior of bare and coated mild steel*

To understand the influence of the biofilm on the biocorrosion process of bare and coated MS, the corrosion products formed under abiotic conditions were analyzed and compared with those formed under biotic conditions (Figure 5). Clearly, in PEI, PEI-ZnO and PEI-CuO, limited corrosion deposits were observed compared to the non-coated steel (Figure 5).

The EDS analysis made over bare and coated MS revealed the presence of Fe, C, and O. In the abiotic medium, the absence of C element on the MS (Figure 5e) is consistent with the absence of bacteria, while its presence over the coated steel is associated to the polymeric coatings (Figure 5f–h). As mentioned above, in the biotic system (Figure 5a–d), the C element present in the bare and coated steel can be associated with SRB biofilm formation (Figure 1a–d), and in the coated samples, with the polymeric matrix from the coating (Figure 1b–d).

The existence of O can be associated with the organics in the polymeric coating, with the ZnO and CuO present in the hybrid coatings (Figure 5c,d,g,h), (Figure 5b–d,f–h), and/or with the existence of corrosion products such as hydroxides or iron oxides (Figure 5) [64]. In addition, EDS analysis clearly shows that Fe is the central element detected as expected considering the substrate composition and corrosion products formed (Figure 5). The overlap of Fe and O elemental distribution with well-defined bright structures in SEM micrographs (Figure 5) suggest that the major corrosion products formed are iron compounds rich in oxygen [65].

To further study the influence of the biofilm in the MIC process of MS, electrochemical impedance spectroscopy (EIS) was used.

Figure 6 shows the Nyquist and Bode plots of the coated steel incubated in ATWW with and without *Desulfovibrio* sp. The increased impedance values compared to the bare MS (Figure S2 in Supplementary Data) indicates higher resistances across the metal/solution electrolyte interface, referring to a higher protection of the steel by the polymetric matrices [66].

In the case of the coated steel immersed for 7 days in the abiotic system, a marked slope associ-

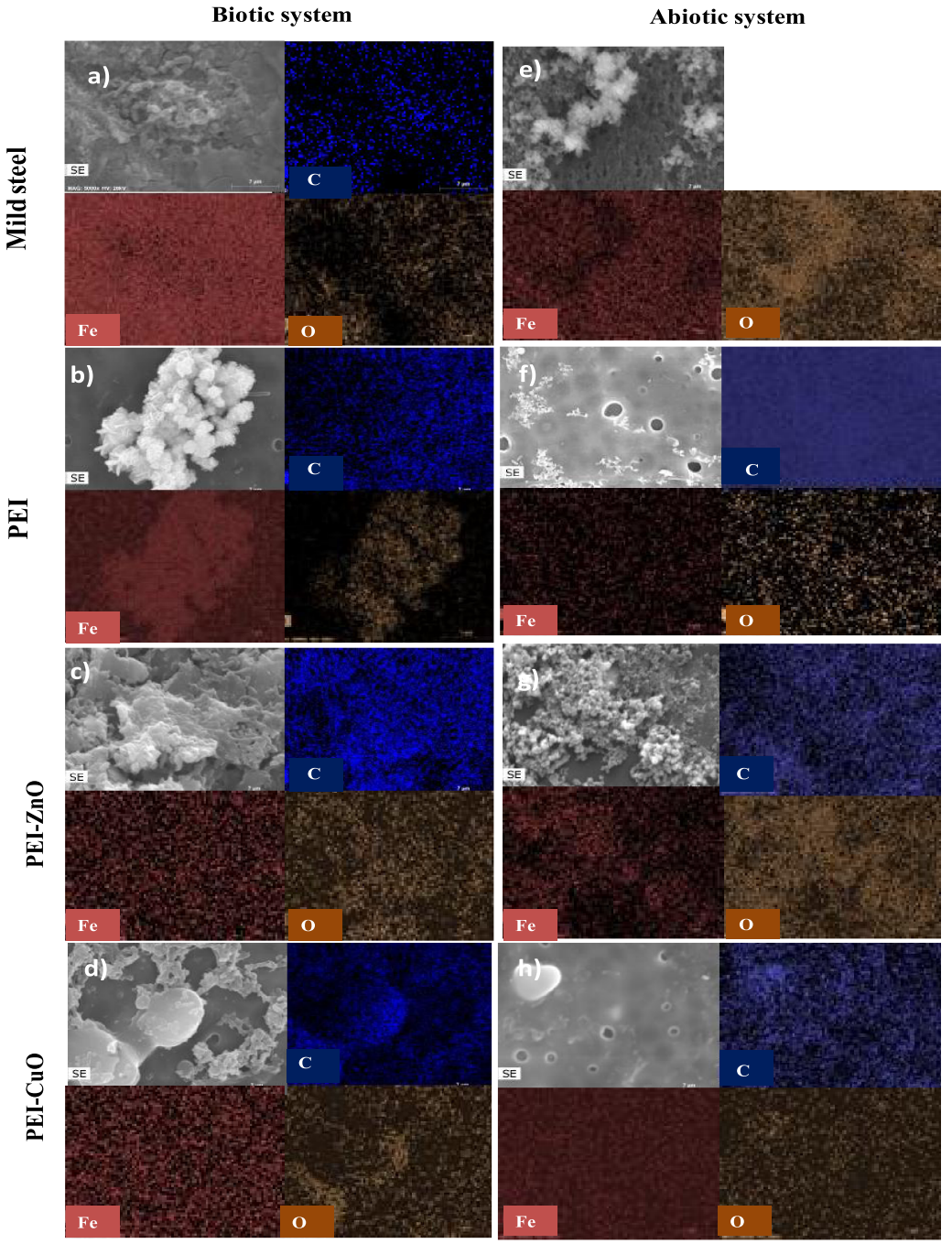

Figure 5. Chemical elements distribution on the coating surface with (a) MS, (b) PEI, (c) PEI-ZnO, (d) PEI-CuO immersed in biotic system, (e) MS, (f) PEI, (g) PEI-ZnO, (h) PEI-CuO immersed 7 days in abiotic system.

ated with a diffusion process is evident in the Nyquist plot, which is associated with the accumulation of the corrosion products (Figure 6a–c). Thus, the EIS spectra can be fitted by the ECC shown in Figure 6d. In the EEC, R_{co} and Q_{co} are the pores resistance and the constant-phase element of the coating layer

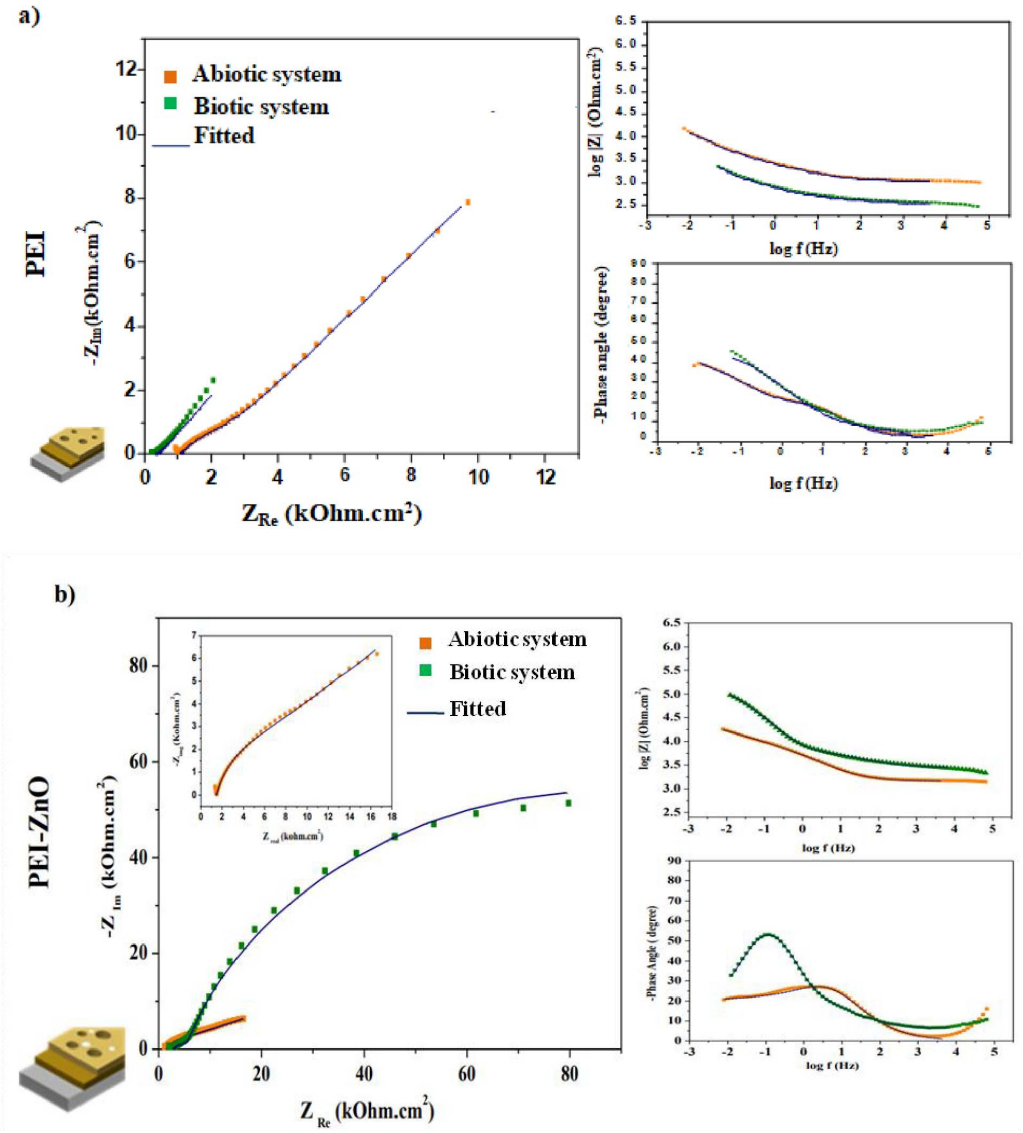

Figure 6. Caption continued on next page.

in the presence of corrosion products, respectively. R_{ct} and Q_{dl} represent the Faradic resistance and double-layer capacitance, whereas W represents the Warburg resistance due to the diffusion process of aggressive ions. This parameter does not exist in the case of a biotic system. The rationale for this can be mass-controlled processes' establishment explained by sealing a portion of pores in the biofilm and the coating. The coating tends to inhibit the growth of *Desulfovibrio* sp, and the weak biofilm layer formed on the coated steel surface might be involved with the corrosion products blocking a part of the pores in the biofilm and coating [67].

In biotic medium, the coated steel showed two-time constants. The first one in the high-frequency range is due to the coating, the biofilm and some corrosion product according to SEM images (Figure 1), and the second constant time, at lower frequencies, can be related to the Faradic responses being at the interface metal/electrolyte (Figure 6) [29].

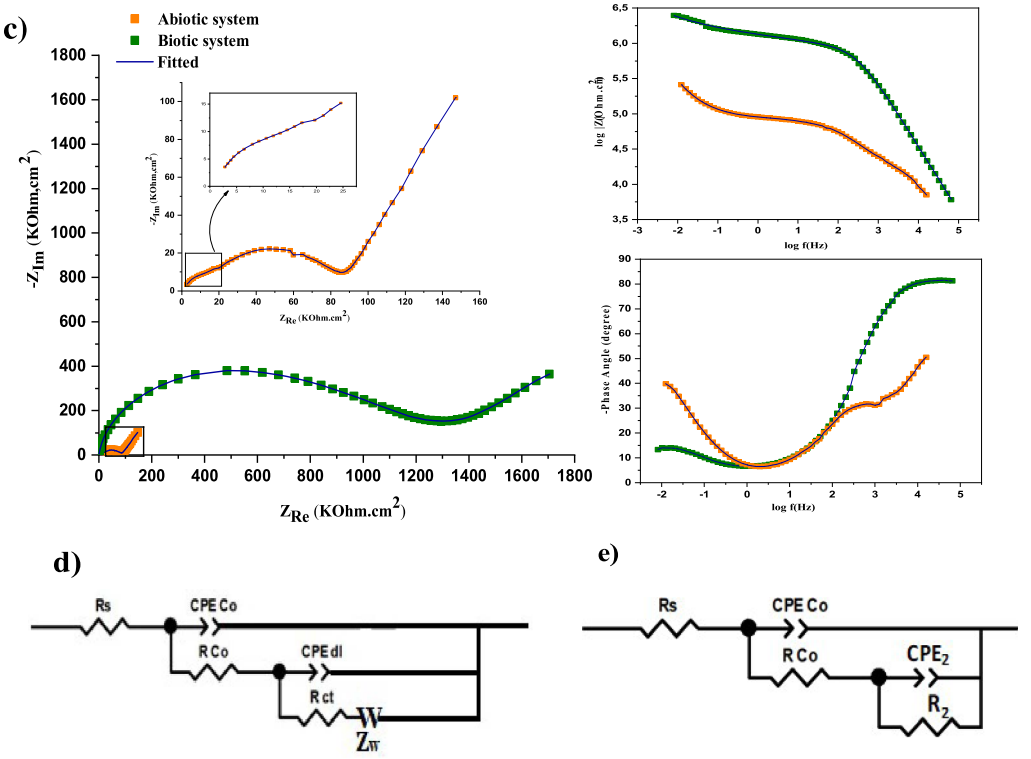

Figure 6 (cont.). Nyquist and Bode plots of coated MS with (a) PEI, (b) PEI-ZnO, and (c) PEI-CuO, (d) the equivalent circuit used to fit the EIS data for the coated MS immersed in abiotic system (ATWW) and (e) the equivalent circuit used to fit the EIS data for the coated MS immersed in biotic system (ATWW + *Desulfovibrio*).

Figure 6e illustrates the EEC used to model the experimental EIS data for the biotic system to calculate the electrochemical parameters at the metal/electrolyte interface. In this case, R_s represents the solution resistance. R_{co} and Q_{co} are the pores resistance and the constant-phase element corresponding coating layer with biofilm and corrosion products, respectively. For the second time constant, R_2 and Q_2 represent the Faradic resistance and double-layer capacitance at the coating/metal interface, respectively. The evolution of the impedance parameters obtained by fitting the experimental results are reported in Table 1. The chi-squared of the regressions, around 10^{-3} and 10^{-4}, indicates good fitting reliability.

As observed in EIS plots of PEI (Figure 6a), a remarkable decrease in the overall impedance was noticed in the presence of the SRB strain. The reduction after 7 immersion days can be attributed to the absence of the protective effect of PEI against the biocorrosion related to the gradual degradation in the protective film (coating and biofilm), which leads to an increased corrosion activity compared to the abiotic system.

According to the EIS spectra (Figure 6b,c), middle and low-frequency time constants observed in PEI-ZnO and PEI-CuO coating present higher impedance values than those of PEI in both biotic and abiotic systems. Indicating higher electrical resistances at the interface of the steels with a solution, and thus decreased corrosion activity.

When comparing the phase angles values for the bare and coated steels after 7 days of immersion, the time constant at high and medium-high frequencies demonstrate that the coatings affect the electrochemical response of the system. More negative phase angle values and increased impedance values for PEI-CuO (Figure 6c) compared to PEI and PEI-ZnO (Figure 6a,b) supported the hypothesis of higher protectiveness of the PEI-CuO coating.

For PEI and PEI-ZnO, the values of log $|Z|$ determined at the lowest frequency are approximately

Table 1. Evolution of the impedance parameters extracted by numerical simulation of the EIS data for the coated mild steel, after 7 days upon immersion in abiotic and biotic systems

Coating	PEI		PEI-ZnO		PEI-CuO	
System incubation	Abiotic	Biotic	Abiotic	Biotic	Abiotic	Biotic
R_s ($\Omega{\cdot}cm^2$)	900	335.8	1459	2815	2616	182.5
R_{co} ($\Omega{\cdot}cm^2$)	1143	142.3	2343	4450	2.6×10^5	6×10^5
Q_{co} ($\Omega^{-1}{\cdot}cm^2{\cdot}s^n$)	1.9×10^{-5}	1.1×10^{-4}	2.3×10^{-5}	1.7×10^{-5}	6.5×10^{-8}	1.1×10^{-9}
n_1	0.55	0.58	0.75	0.59	0.62	0.9
R_2 ($\Omega{\cdot}cm^2$)	7544	1554	9754	1.5×10^5	6.3×10^5	2.2×10^6
Q_{dl} ($\Omega^{-1}{\cdot}cm^2{\cdot}s^n$)	7.6×10^{-5}	3×10^{-4}	6.5×10^{-5}	2.9×10^{-5}	8×10^{-6}	6.5×10^{-7}
n_2	0.68	0.59	0.86	0.56	0.77	0.48
W	3×10^{-4}	—	1.2×10^{-8}	—	2.5×10^{-6}	—
χ^2	7.6×10^{-3}	3×10^{-4}	$1.5\times10^{-.3}$	1.9×10^{-3}	2×10^{-4}	1.5×10^{-3}

2.8×10^3 and 9.5×10^4 $\Omega{\cdot}cm^2$, respectively (Figure 6a and b). In contrast, in the PEI-CuO coating, values were of 2.5×10^6 $\Omega{\cdot}cm^2$ (Figure 6c). Thus, the PEI-CuO shows higher efficiency as an anti-corrosive coating in three systems: chloride medium [29], abiotic system (SATWW) and biotic system (ATWW in the presence of *Desulfovibrio* sp.), probably due to the higher coating thickness and decreased porosity in the outer layer [29].

As shown in Figure 6b,c, in the biotic system, the impedance values are notably higher than abiotic ones demonstrating that PEI-metal oxides resulted in a biocorrosion inhibition.

The variation of R_{co} and R_2 (R_{ct} in the case of the abiotic system) in different media for the different coating is shown in Figure S3(a,b) and (c,d). R_{co} and R_2 increased with the presence of ZnO and CuO in the abiotic medium (Figure S3b–d), which led to the gradual formation of a protective corrosion product film that decreased the corrosion of MS. Besides, the PEI and PEI-ZnO coatings have the lowest resistance compared to the PEI-CuO, which shows the rapid degradation of the film and,consequently, the corrosion increases.

In the case of hybrid coatings, the values of R_{co} and R_2 in biotic medium were larger than in the abiotic medium. The increase in the biolayer thickness and the lower metabolic activity of SRB can explain these values. The effectiveness of PEI-CuO may also be related to the higher thickness (51 μm) and the limited number of holes formed before and after immersion in the aggressive medium. Despite the similar thickness value observed for PEI-ZnO and PEI (43 μm) [29], a sharp decrease of R_{co} and R_2 was observed for PEI in the biotic system. This behavior may be related to a high concentration of corrosive metabolites from bacteria.

Whatever the immersion medium, PEI-CuO had the highest efficiency (Figure S3 in Supplementary Data) when compared with the other coatings. These results may be related to the increased thickness, the decreased porosity [29] and/or the composition of the produced EPS (biotic system). Moreover, as a nobler alloying element, Cu protects steel by suppressing anodic dissolution [68]. The percentages of protection efficiency increased in the presence of *Desulfovibrio* sp. for PEI-CuO and PEI-ZnO coatings, indicating that the biofilm formed on the surface of the PEI-metal oxide coatings has a protective role against biocorrosion.

Various factors can influence the biocorrosion process, such as biofilm structure, surface coverage and EPS composition [69]. For uncoated and PEI-coated MS, the microbial presence accelerates the biocorrosion rate by creating different electrochemical potentials (Figure S4) [70]. According to Miranda *et al.* [10], the existence of *Desulfovibrio* sp on the steel surface results in a deposition of ferric sulfates. Microbial clusters result in anaerobic microenvironments beneath the deposits, producing conditions for the accumulation of Cl^- that combine with iron to form acidic ferric chloride. Generally, these compounds are highly corrosive to steels. In addition, the presence of sulfides can induce pitting on steel [15].

According to Mostafaei *et al.* [71], after immersion, ZnO and CuO reduction within coatings leads to the release of Zn^{2+} and Cu^{2+}. These ions interact with polymers' nitrogen atoms and form compact clusters that increase the electron-rich benzenoid groups to facilitate a greater coverage on the metal surface. Consequently, a delay diffusion of O_2, H_2O, and Cl^- occurs on the steel surface [29]. In the biotic system, the biofilm formed on the surface of the composite coating increases the corrosion resistance of MS. In fact, the protective role of the bacterial biofilm [72] is confirmed to be a function of its bacterial diversity, which influences the biofilm attachment, EPS composition, biofilm thickness, density, and metal chelation [26]. In this context, the corrosion protection by the biofilm seems to be enhanced by bacterial strains such as *vibrio* and *Serratia marcescens EF190* are used. The formation of a protective layer on the steel surface, in the first step of attachment, was demonstrated along side oxygen consumption by electron transports proteins [23,70].

Moreover, biofilm development and its properties are highly influenced by the composition of extracellular polymeric substances (EPS) [17,23,73]. Corrosion inhibition by these proteins have been demonstrated earlier [74–76]. Due to their stable adsorption, proteins interact with metal ions (Zn^{2+} and Cu^{2+}) and create metal-protein complexes (chelates) on the steel surface. This reaction helps to decrease the metal release, blocking other mechanisms such as electrochemical dissolution and, therefore slowing down corrosion. Moreover, exopolysaccharides were reported to be used for corrosion protection. Scheerder *et al.* [77] reported that when the first step (Figure S5) of corrosion takes place, Fe^{2+} can interact with –C–OH, $–CH_3$, $–CH_2–$ and $–COO^-$ in the polysaccharide and –C=O– and –COO– in the protein molecules. As such, these ions can no longer participate in the electrochemical process. Because it is not soluble in the coating matrix, the metal complex will likely deposit at the coating-metal interface. Thus, such metal complexes will form a protective layer on the steel surface, preventing the diffusion of corrosive particles and oxygen dissolved. Under this layer, the probability of Fe^{2+} binding with H_2O, O_2, and polysaccharide/protein molecules is reduced, the resistance is gradually increased, and corrosion is inhibited.

4. Conclusion

A new approach to reduce biocorrosion induced by *Desulfovibrio* sp. using new hybrid coatings for MS protection in ATWW was achieved with PEI-ZnO and PEI-CuO coatings. The bare steel surface had an adherent homogeneous biofilm, confirming that the biofilm can quickly be established upon SRB colonization. In PEI-coated MS, fewer and scattered bacterial colonies developed on the metal surface, either in separate colonies or small clusters. The PEI coating makes it difficult for bacteria to colonize and access MS surface under coating and PEI-ZnO and PEI-CuO coatings led to a more heterogeneous biofilm structure. A pronounced bactericide effect was depicted for PEI-ZnO and PEI-CuO coatings, with the number of SRB individual colonies significantly decreasing with a more intricate porous structure. From these two coatings, higher protein content, from the EPS characterization occurred in the presence of the PEI-CuO coating. EIS measurements in the biotic medium showed that the hybrid coatings, PEI-ZnO and PEI-CuO, significantly increased the protection of MS against biocorrosion compared to PEI coatings. The biofilm itself acted as a protective film, showing increased resistance values for the ZnO and CuO modified coatings. PEI-CuO seemed more protective, either in the absence or presence of bacteria, where PEI seemed to act as anti-adherent agent and CuO as antimicrobial agent. Moreover, EPS extracted from the biofilm formed on the PEI-CuO surface can be suggested as a green biocorrosion inhibitor in wastewater.

Conflicts of interest

Authors have no conflict of interest to declare.

Acknowledgments

The authors would like to gratefully express their appreciation to the Tunisian Ministry of Higher Education and Scientific Research and the Fundação para a Ciência e Tecnologia (FCT) through the project UIDB/00100/2020, IDB/00100/2020, UIDP/00100/2020, LA/P/0056/2020 for the financial support.

Supplementary data

Supporting information for this article is available on the journal's website under https://doi.org/10.5802/crchim.227 or from the author.

References

[1] H. Zhang, Y. Tian, J. Wan, P. Zhao, *Appl. Surf. Sci.*, 2015, **357**, 236-247.

[2] P. Cantinho, M. Matos, M. A. Trancoso, M. M. C. dos Santos, *Int. J. Environ. Sci. Technol.*, 2016, **13**, 359-386.

[3] L. Abdoli, X. Suo, H. Li, *Colloids Surf. B*, 2016, **145**, 688-694.

[4] H. Wang, M. Sodagari, Y. Chen, X. He, B.-M. Z. Newby, L.-K. Ju, *Colloids Surf. B*, 2011, **87**, 415-422.

[5] D. Starosvetsky, R. Armon, J. Yahalom, J. Starosvetsky, *Int. Biodeterior. Biodegrad.*, 2001, **47**, 79-87.

[6] F. Batmanghelich, L. Li, Y. Seo, *Corros. Sci.*, 2017, **121**, 94-104.

[7] V. S. Liduino, M. T. S. Lutterbach, E. F. C. Sérvulo, *Colloids Surf. B*, 2018, **172**, 43-50.

[8] T. Wu, M. Yan, L. Yu, H. Zhao, C. Sun, F. Yin, W. Ke, *Corros. Sci.*, 2019, **157**, 518-530.

[9] H. Liu, Y. F. Cheng, *Electrochim. Acta*, 2017, **253**, 368-378.

[10] E. Miranda, M. Bethencourt, F. J. Botana, M. J. Cano, J. M. Sánchez-Amaya, A. Corzo, J. G. De Lomas, M. L. Fardeau, B. Ollivier, *Corros. Sci.*, 2006, **48**, 2417-2431.

[11] K. Rasool, A. Shahzad, D. S. Lee, *J. Hazard. Mater.*, 2016, **318**, 641-649.

[12] I. Ziadi, M. M. Alves, M. Taryba, L. El-Bassi, L. Bousselmi, M. F. Montemor, H. Akrout, *Bioelectrochemistry*, 2020, **132**, article no. 107413.

[13] B. Wei, J. Xu, Q. Fu, Q. Qin, Y. Bai, C. Sun, C. Wang, Z. Wang, W. Ke, *J. Mater. Sci. Technol.*, 2021, **87**, 1-17.

[14] S. Q. Chen, P. Wang, D. Zhang, *Mater. Corros.*, 2016, **67**, 340-351.

[15] Y. Li, S. Feng, H. Liu, X. Tian, Y. Xia, M. Li, K. Xu, H. Yu, Q. Liu, C. Chen, *Corros. Sci.*, 2020, **167**, article no. 108512.

[16] L. El-Bassi, I. Ziadi, S. Belgacem, L. Bousselmi, H. Akrout, *Int. Biodeterior. Biodegrad.*, 2020, **150**, article no. 104960.

[17] P. Rajala, E. Huttunen-Saarivirta, M. Bomberg, L. Carpén, *Corros. Sci.*, 2019, **159**, article no. 108148.

[18] R. Jia, J. L. Tan, P. Jin, D. J. Blackwood, D. Xu, T. Gu, *Corros. Sci.*, 2018, **130**, 1-11.

[19] U. Eduok, E. Ohaeri, J. Szpunar, *Mater. Sci. Eng. C*, 2019, **105**, article no. 110095.

[20] A. J. Wikie, I. Datsenko, M. Vera, W. Sand, *Bioelectrochemistry*, 2014, **97**, 52-60.

[21] G. Hwang, S. Kang, M. G. El-Din, Y. Liu, *Colloids Surf. B*, 2012, **91**, 181-188.

[22] K. Sauer, *Genome Biol.*, 2003, **4**, 1-5.

[23] N. Jacob, R. Radhakrishnan, V. Sunil, G. Kamalanathan, A. Sengupta, R. Wickramasinghe, *Sep. Purif. Technol.*, 2018, **205**, 32-47.

[24] R. Babaei-Sati, J. Basiri Parsa, M. Vakili-Azghandi, *Synth. Met.*, 2019, **247**, 183-190.

[25] A. Mathur, M. Bhuvaneshwari, S. Babu, N. Chandrasekaran, A. Mukherjee, *J. Environ. Chem. Eng.*, 2017, **5**, 3741-3748.

[26] C. M. Cordas, L. T. Guerra, C. Xavier, J. J. G. Moura, *Electrochim. Acta*, 2008, **54**, 29-34.

[27] I. B. Beech, V. Zinkevich, R. Tapper, R. Gubner, R. Avci, *J. Microbiol. Methods*, 1999, **36**, 3-10.

[28] C. C. C. R. de Carvalho, *Front. Mar. Sci.*, 2018, **5**, 1-11.

[29] E. Rahali, M. M. Alves, L. El-Bassi, L. Bousselmi, M. F. Montemor, H. Akrout, *Prog. Org. Coat.*, 2022, **163**, article no. 106602.

[30] I. Ziadi, L. El-Bassi, L. Bousselmi, H. Akrout, *Biofouling*, 2020, **36**, 977-989.

[31] H. Liu, H. H. P. Fang, *J. Biotechnol.*, 2002, **95**, 249-256.

[32] M. Dubois, K. A. Gilles, J. K. Hamilton, P. A. Rebers, F. Smith, *Anal. Chem.*, 1956, **28**, 350-356.

[33] Y. Lin, M. de Kreuk, M. C. M. van Loosdrecht, A. Adin, *Water Res.*, 2010, **44**, 3355-3364.

[34] C. S. Frings, T. W. Fendley, R. T. Dunn, C. A. Queen, *Clin. Chem.*, 1972, **18**, 673-674.

[35] K. Rasool, G. K. Nasrallah, N. Younes, R. P. Pandey, P. A. Rasheed, K. A. Mahmoud, *ACS Sustain. Chem. Eng.*, 2018, **6**, 3896-3906.

[36] J. Aguirre, L. Daille, D. A. Fischer, C. Galarce, G. Pizarro, I. Vargas, M. Walczak, R. de la Iglesia, F. Armijo, *Prog. Org. Coat.*, 2017, **113**, 175-184.

[37] P. A. Rasheed, K. A. Jabbar, K. Rasool, *Corros. Sci.*, 2019, **148**, 397-406.

[38] L. K. Adams, D. Y. Lyon, P. J. J. Alvarez, *Water Res.*, 2006, **40**, 3527-3532.

[39] M. Malini, M. Thirumavalavan, W. Y. Yang, J. F. Lee, G. Annadurai, *Int. J. Biol. Macromol.*, 2015, **80**, 121-129.

[40] G. S. Dhillon, S. Kaur, S. K. Brar, *Int. Nano Lett.*, 2014, **4**, 1-11.

[41] L. E. Shi, Z. H. Li, W. Zheng, Y. F. Zhao, Y. F. Jin, Z. X. Tang, *Food Addit. Contam. — Part A Chem. Anal. Control. Expo. Risk Assess.*, 2014, **31**, 173-186.

[42] X. He, G. Zhang, X. Wang, R. Hang, X. Huang, L. Qin, B. Tang, X. Zhang, *Ceram. Int.*, 2017, **43**, 16185-16195.

[43] Z. Chen, S. Gao, M. Jin, S. Sun, J. Lu, P. Yang, P. L. Bond, Z. Yuan, J. Guo, *Environ. Int.*, 2019, **125**, 65-74.

[44] K. Alasvand Zarasvand, V. R. Rai, *3 Biotech*, 2016, **6**, 1-7.

[45] M. Fathy, A. Badawi, A. M. Mazrouaa, N. A. Mansour, E. A. Ghazy, M. Z. Elsabee, *Mater. Sci. Eng. C*, 2013, **33**, 4063-4070.

[46] L. Dyshlyuk, O. Babich, S. Ivanova, N. Vasilchenco, V. Atuchin, I. Korolkov, D. Russakov, A. Prosekov, *Int. Biodeterior. Biodegrad.*, 2020, **146**, article no. 104821.

[47] A. Sirelkhatim, S. Mahmud, A. Seeni, N. H. M. Kaus, L. C. Ann, S. K. M. Bakhori, H. Hasan, D. Mohamad, *Nano-Micro Lett.*, 2015, **7**, 219-242.

[48] L. Boulangé-Petermann, J. Rault, M. N. Bellon-Fontaine, *Biofouling*, 1997, **11**, 201-216.

[49] H. M. Dalton, L. K. Poulsen, P. Halasz, M. L. Angles, A. E. Goodman, K. C. Marshall, *J. Bacteriol.*, 1994, **176**, 6900-6906.

[50] S. Chen, Y. Li, Y. F. Cheng, *Sci. Rep.*, 2017, **7**, 1-9.

[51] Z. Wang, Y. Su, Q. Li, Y. Liu, Z. She, F. Chen, L. Li, X. Zhang, P. Zhang, *Mater. Charact.*, 2015, **99**, 200-209.

[52] I. Ziadi, H. Akrout, H. Hassairi, L. El-Bassi, L. Bousselmi, *Eng. Fail. Anal.*, 2019, **101**, 342-356.

[53] W. Artifon, S. M. Pasini, A. Valério, S. Y. G. González, S. M. de Arruda Guelli Ulson de Souza, A. A. U. de Souza, *Mater. Sci. Eng. C*, 2019, **103**, article no. 109859.

[54] E. H. Hewayde, G. F. Nakhla, E. N. Allouche, P. K. Mohan, *Struct. Infrastruct. Eng.*, 2007, **3**, 267-277.

[55] H. H. P. Fang, L. C. Xu, K. Y. Chan, *Water Res.*, 2002, **36**, 4709-4716.
[56] L. Miao, C. Wang, J. Hou, P. Wang, Y. Ao, Y. Li, Y. Yao, B. Lv, Y. Yang, G. You, Y. Xu, Q. Gu, *Sci. Total Environ.*, 2017, **579**, 588-597.
[57] Z. Yue, Q. Li, C. Li, T. Chen, J. Wang, *Bioresour. Technol.*, 2015, **194**, 399-402.
[58] J. Zhao, S. Liu, N. Liu, H. Zhang, Q. Zhou, F. Ge, *Sci. Total Environ.*, 2019, **658**, 582-589.
[59] E. J. Pérez, R. Cabrera-Sierra, I. González, F. Ramírez-Vives, *Corros. Sci.*, 2007, **49**, 3580-3597.
[60] J. Hou, L. Miao, C. Wang, P. Wang, Y. Ao, B. Lv, *Bioresour. Technol.*, 2015, **176**, 65-70.
[61] A. Conrad, M. Kontro, M. M. Keinänen, A. Cadoret, P. Faure, L. Mansuy-Huault, J. C. Block, *Lipids*, 2003, **38**, 1093-1105.
[62] M. E. Davey, G. A. O'toole, *Microbiol. Mol. Biol. Rev.*, 2000, **64**, 847-867.
[63] H. Liu, H. H. P. Fang, *Biotechnol. Bioeng.*, 2002, **80**, 806-811.
[64] S. Gao, B. Brown, D. Young, M. Singer, *Corros. Sci.*, 2018, **135**, 167-176.
[65] H. Liu, C. Fu, T. Gu, G. Zhang, Y. Lv, H. Wang, H. Liu, *Corros. Sci.*, 2015, **100**, 484-495.
[66] S. Chongdar, G. Gunasekaran, P. Kumar, *Electrochim. Acta*, 2005, **50**, 4655-4665.
[67] E. Ilhan-Sungur, T. Unsal-Istek, N. Cansever, *Mater. Chem. Phys.*, 2015, **162**, 839-851.
[68] Y.-W. Jang, J.-H. Hong, J.-G. Kim, *Met. Mater. Int.*, 2009, **15**, 623-629.
[69] Z. Guo, T. Liu, Y. F. Cheng, N. Guo, Y. Yin, *Colloids Surf. B*, 2017, **157**, 157-165.
[70] Y. Chen, Q. Tang, J. M. Senko, G. Cheng, B. Min Zhang Newby, H. Castaneda, L. K. Ju, *Corros. Sci.*, 2015, **90**, 89-100.
[71] A. Mostafaei, F. Nasirpouri, *Prog. Org. Coat.*, 2014, **77**, 146-159.
[72] A. Pedersen, S. Kjelleberg, M. Hermansson, *J. Microbiol. Methods*, 1988, **8**, 191-198.
[73] M. Moradi, Z. Song, X. Tao, *Electrochem. Commun.*, 2015, **51**, 64-68.
[74] T. Rabizadeh, S. K. Asl, *J. Mol. Liq.*, 2019, **276**, 694-704.
[75] F. Zhang, J. Pan, P. M. Claesson, *Electrochim. Acta*, 2011, **56**, 1636-1645.
[76] M. Talha, Y. Ma, P. Kumar, Y. Lin, A. Singh, *Colloids Surf. B*, 2019, **176**, 494-506.
[77] J. Scheerder, R. Breur, T. Slaghek, W. Holtman, M. Vennik, G. Ferrari, *Prog. Org. Coat.*, 2012, **75**, 224-230.